JOURNAL OF APPLIED ELECTROCHEMISTRY 23 (1993) 662–668

Transition layer thickness in microlaminar deposits*

A. R. DESPIĆ, T. LJ. TRIŠOVIĆ

Institute of Technical Sciences of the Serbian Academy of Science and Arts, P.O. Box 745, 11000 Belgrade, Yugoslavia

Received 10 February 1992; revised 20 August 1992

A theoretical analysis was carried out on the change of composition of a deposit obtained by the dual pulse method of forming laminar metal foils, with transition from a low current to a high current pulse, both in the galvanostatic and the potentiostatic mode of deposition. It was shown that the existence of a transition layer of varying composition between a layer of pure metal 1 and a layer consisting predominantly of the metal 2 is an inherent consequence of the electrochemical process, primarily because of an induction period in the concentration polarization with respect to ions of metal 1. The importance of this transition layer increases as the thickness of the layers of the two metals decreases. Eventually this limits the possibility of obtaining a sharp boundary between the layers, when the nanometre region of layer thickness is reached. Equations are given for calculating the deposition current density and rate of stirring of the electrolyte which provide a deposit of a required level of metal 1 in the layer of metal 2, as well as a required sharpness of the boundary between two layers. Experimental proof of the correctness of the analysis was sought. It was found that significant changes in the properties of the deposit occur in the same range of layer thickness in which the transition of the composition takes places.

Nomenclature

$\alpha_{c,1}$, $\alpha_{c,2}$	transfer coefficient of the cathodic processes
C	interfacial capacitance
C_1, C_2	concentration of the ions of metals 1 and 2 at the interface r
C_1^0, C_2^0	concentration of ions of the metals 1 and 2 in solution
D_1	diffusion coefficient for the diffusion of ions of the metal 1
$E_{r,1}$, $E_{r,2}$	reversible potentials of metals 1 and 2, respectively
F	the Faraday constant
J_1^0, J_2^0	exchange current density of the metals 1 and 2, respectively
M_1, M_2	atomic weights of the metals 1 and 2, respectively
ν	kinematic viscosity of solution
ρ_1, ρ_2	densities of the metals 1 and 2 respectively
v	rotation speed (r.p.s.)
z	number of electrons exchanged in the deposition process

1. Introduction

In recent years an electrochemical method has been derived for obtaining laminar metal coatings and foils from a single electrolyte bath [1–7]. Such coatings comprise a multitude of layers of two different metals (e.g. copper and nickel) deposited upon each other. This can be achieved by applying a pulsating regime of electrodeposition consisting of the application of trains of single or dual pulses of current (low and high) or potential (less and more negative than those needed for depositing both metals), with a possible addition of pulsating hydrodynamics in the solution [6].

A theory was developed defining conditions of current (or potential) in the pulses, as well as of pulse duration needed to obtain layers of desired thickness of metal 1 and metal 2. The theory also took note of the desired content of metal 1 in the layer of metal 2, since the latter cannot be obtained free of some amount of the former [4, 5]. It was assumed that the change of current or potential driving the metal deposition processes is instantaneous; i.e. instantaneous regardless of whether in the galvanostatic or potentiostatic mode. This assumption was shown to be valid for relatively thick layers of the order of a micrometre, as X-ray analysis or microscopic observations revealed sharp boundaries between them [5].

Some work, however, indicated that it is the domain of very thin layers (in the nanometre range) which may be of interest for obtaining materials with properties superior to those of both parent metals [7]. Hence, a significant amount of research is currently being undertaken in the field. However, even the most sophisticated techniques available make it difficult to discern between layers of such thickness. In the present communication an attempt was made to analyse to what extent,

*This paper is dedicated to Professor Brian E. Conway on the occasion of his 65th birthday, and in recognition of his outstanding contribution to electrochemistry.

0021-891X/93

and down to which layer thicknesses, the electrochemical deposition can give layers of relatively constant composition justifying the description of the deposit as laminar compared with those with periodically varying composition.

Further, equations based on well-established electrochemical kinetic relationships are developed which enable calculation of the process parameters necessary to obtain deposits of required quality.

2. Theoretical considerations

2.1. *Derivation of the deposition kinetics*

Processes taking place at an interface between a conducting substrate and an electrolyte determine the relationship between the passage of electric current, J, and the change of electric potential across the interface, E, in a manner analogous to that in the electric circuit shown in Fig. 1. Here C is the interfacial capacitance. $R_{f,1}$ and $R_{f,2}$ are complex 'faradaic' (non-linear) resistances reflecting the rates of deposition of metals 1 and 2, respectively, while R_Ω is the ohmic resistance of the electrolyte between the electrode surface and a point at which the other end of the potential difference E is measured (usually the tip of the Luggin capillary).

The current, J, is a sum of three partial currents:
(i) The capacitance current, J_c, arises when the potential E' is changed and is given by

$$J_c = -C(\mathrm{d}E'/\mathrm{d}t) \tag{1}$$

Note that the minus sign arises in order to obtain a positive value of the current as the potential is driven in the negative direction.
(ii) The faradaic current resulting in deposition of the metal 1 is given by the well known equation of electrode kinetics

$$J_1 = J_1^0(C_1/C_1^0)\exp\left[-(\alpha_{c,1}F/RT)(E' - E_{r,1})\right] \tag{2}$$

(assuming that $(E' - E_{r,1})$ is sufficiently large that the rate of anodic dissolution of the metal 1 is negligible),
(iii) A similar equation applies to the deposition of the metal 2, i.e.

$$J_2 = J_2^0(C_2/C_2^0)\exp\left[-(\alpha_{c,2}F/RT)(E' - E_{r,2})\right] \tag{3}$$

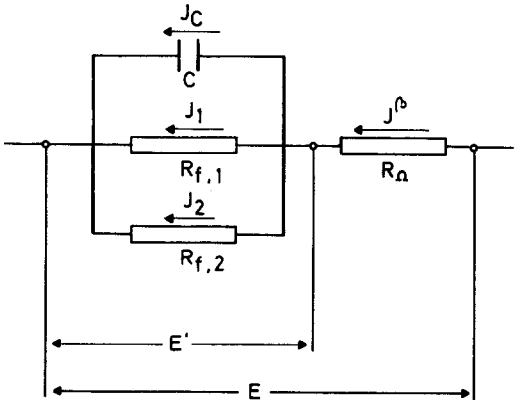

Fig. 1. Equivalent circuit for electrochemical deposition of two different metals from solutions containing their cations.

The potential E', across the interface is related to the measurable (and controllable) potential E by

$$E' = E + R_\Omega J \tag{4}$$

The above equations are applicable to any regime of current or potential. Two regimes used in practice for obtaining laminar deposits are analysed here. These are the dual-pulse galvanostatic and dual-pulse potentiostatic regimes.

2.1.1. Galvanostatic mode of operation: Galvanostatic deposition is characterized by two levels of constant current J^α and J^β. The first current is adjusted so as not to cause significant concentration polarization with respect to deposition of metal 1, i.e. $(C_1/C_1^0) \approx 1$ at any time during the first period. Hence, pure metal 1 is deposited at a rate J_1 equal to J^α, since at the potential corresponding to J_1, the current J_2 is negligible. The potential E, which is needed to drive J_1 is given by Equation 2 combined with Equation 4.

When the current is stepped-up to J^β two phenomena arise: (i) the potential E' lags behind this change, because of the need to charge the interfacial capacitance, C, to a new value of potential required to give the partial currents new intensities adding up to J^β at steady state; (ii) as J_1 and J_2 rise, the concentration of the depositing ions at the interface, and in particular C_1, begin to decrease.

Assuming that the ions reach the surface by molecular diffusion from an infinitely large bulk of immobile solution, the concentration change, for example of the ions of metal 1, can be described [8] by

$$(C_1/C_1^0) = 1 - (2t^{1/2}/zF\pi^{1/2}D_1^{1/2}C_1^0)J_1 \tag{5}$$

Note that Equation 5 is derived for the case of constant current, but is also applicable to a current changing with time.

A similar equation should apply to C_2/C_2^0. However, at this point it will be assumed that C_2^0 is so much larger than C_1^0 that this ratio stays unity during the pulse, as is usually the case.

Inserting Equation 5 into Equation 2 and rearranging, gives

$$J_1 = \frac{J_1^0 \exp\left[-\left(\frac{\alpha_{c,1}F}{RT}\right)(E' - E_{r,1})\right]}{1 + 2\left(\frac{t^{1/2}}{zF\pi^{1/2}D_1^{1/2}C_1^0}\right)J_1^0 \exp\left[-\left(\frac{\alpha_{c,1}F}{RT}\right)(E' - E_{r,1})\right]} \tag{6}$$

It should be noted that, at increasing time of deposition and as the second term in the denominator becomes much larger than 1, the current becomes entirely diffusion controlled, that is

$$J_1 = zF\pi^{1/2}D_1^{1/2}C_1^0/2t^{1/2} \tag{7}$$

The current J_1 would continue decreasing if the diffusion layer did not reach a hydrodynamic layer boundary, at a certain distance δ_d, beyond which the concentration remains C_1^0 at all times, due to the

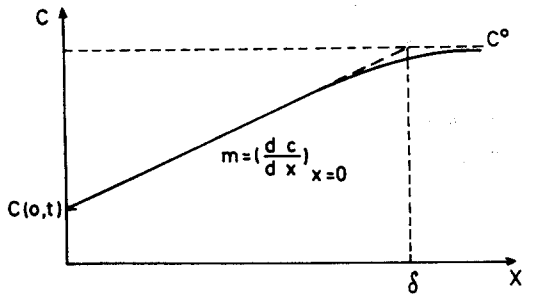

Fig. 2. Schematic representation of the concentration profile of ions in the diffusion layer at an electrode/solution interface. δ: Nernst diffusion layer thickness.

motion of the solution. If the Nernst concept of the diffusion layer is assumed, as shown schematically in Fig. 2, the diffusion layer thickness δ is

$$\delta = D_1[C_1^0 - C_1]/(\mathrm{d}C_1/\mathrm{d}x)_{x=0} = zFD[C_1^0 - C_1]/J_1 \tag{8}$$

Inserting Equations 5 and 6 into Equation 8 it can be seen that

$$\delta = 2D_1^{1/2}t^{1/2}/\pi^{1/2} \tag{9}$$

In other words the diffusion layer thickness is independent of the current density and depends only on time. Thus, it may be solved for the time, τ, at which J_1 attains a steady state value, as

$$\tau = (\pi/4D_1)\delta_d^2 \tag{10}$$

For example a rotating disc cathode δ_d is given by the Levich equation

$$\delta_d = 0.644D_1^{1/3}\nu^{1/6}v^{-1/2} \tag{11}$$

Inserting Equation 11 into Equation 10 gives

$$\tau = 0.325D_1^{-1/3}\nu^{1/3}v^{-1} \tag{12}$$

The overall current–potential relation can be obtained by summing-up Equations 1, 2 and 3 with Equations 4 and 5 inserted, that is,

$$\begin{aligned} J^\beta = &- C\,\mathrm{d}(E + R_\Omega J^\beta)/\mathrm{d}t + J_1^0 \\ &\times \exp[(\alpha_{c,1}F/RT)(E_{r,1})] \\ &\times \exp[-(\alpha_{c,1}F/RT)(E + R_\Omega J^\beta)]/ \\ &\{1 + (2t^{1/2}/zF\pi^{1/2}D_1^{1/2}C_1^0)J_1^0 \\ &\times \exp[(\alpha_{c,1}F/RT)E_{r,1}] \\ &\times \exp[-(\alpha_{c,1}F/RT)(E + R_\Omega J^\beta)]\} \\ &+ J_2^0 \exp[(\alpha_{c,2}F/RT)E_{r,2}] \\ &\times \exp[-(\alpha_{c,2}F/RT)(E + R_\Omega J^\beta)] \end{aligned} \tag{13}$$

To obtain the potential E as a function of time for a constant J^β in the pulse, Equation 13 must be integrated from $t = 0$ at the beginning of the second current step and from a corresponding initial potential E^α. Note that the character of Equation 13 requires that, at $t = 0$, some current J^α must flow through the system in order to obtain a finite value of E^α from which the charging starts as a current step J^β is introduced.

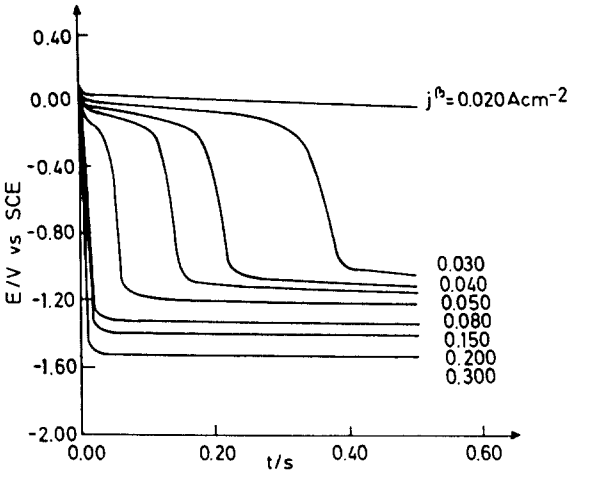

Fig. 3. The calculated change of potential with time during galvanostatic deposition of two metal layers upon each other from a single electrolyte at different cathodic current densities (assumed parameters of the processes cited in Table 1).

Table 1. Parameters used in computing the current–potential relationships in the galvanostatic mode of operation

Parameter	*Numerical value and unit*
Exchange current density, J_1^0	10^{-2} A cm^{-2}
Exchange current density, J_2^0	10^{-4} A cm^{-2}
Transfer coefficient, $\alpha_{c,1} = \alpha_{c,2}$	0.5
Kinematic viscosity, ν	10^{-2} cm^2 s^{-1}
Equilibrium potential, $E_{r,1}$	0.1 V
Equilibrium potential, $E_{r,2}$	−0.8 V
Diffusion coefficient, D	10^{-4} cm^2 s^{-1}
Bulk concentration of ions of the metal 1, C_1^0	10^{-5} mol cm^{-3}
Interfacial capacitance, C	10^{-4} F cm^{-2}
Ohmic resistance, R_Ω	1 Ω cm^2

Such an integration was performed by computer. Figure 3 demonstrates an example derived for the potential–time relationship with the parameters listed in Table 1, expected for the Cu/Ni system: and with J^β varying between 20 and 300 mA cm^{-2}.

The current J^α was made very small compared to J^β so that $E^\alpha = E_{r,1}$. It is seen that the transients correspond to typical galvanostatic charging curves at currents which cause total concentration polarization with respect to the first reducible ion. Fig. 4 shows the change in the partial currents with time. It is seen (Fig. 4a) that, for a reasonable value of the interfacial capacitance, the capacitance current J_c, subsides after a very short time of the order of milliseconds. Subsequent humps reflect further charging of the double layer for the transition from the deposition of the metal 1 towards deposition of the metal 2.

It should be noted that the quantity of electricity spent on metal deposition within the charging time, obtained by integration of the two partial currents J_1 and J_2, indicates that less than a monolayer of metal is deposited.

Hence, it may be concluded that, unless some unusual pseudo-capacitances appear at the interface, the capacitance current, as a factor decreasing the deposition current within one and the same J^β, has

little effect on the deposition process.

The partial currents of metal deposition, J_1 and J_2 are seen in Fig. 4(b) and (c), to change during a substantially longer period of time during which a layer of changing composition is formed (transition layer).

Except for the lowest current density the current J_1 is seen to become diffusion controlled (and is thus independent of total current) after different time intervals corresponding to different transition times.

2.1.2. Potentiostatic mode: If the electrode potential is stepped up and down between two values E_1 and E_2, using a fast potentiostat, the entire change does not immediately settle across the interface. On the contrary, at the beginning of the step the entire change is used to drive the current through the ohmic resistance R_Ω in order to charge the capacitance, and thus change the potential. Hence, the initial current is determined as

$$J^\beta(0) = [(E_2 - E_1)/R_\Omega] + J^\alpha \tag{14}$$

As the capacitance is being charged, E' begins to deviate from the value driving the current J^α, towards $E_2 + R_\Omega J^\beta$ and the faradaic processes start changing their rates.

Equations 1 to 4 also describe the situation in this case, except that now $E = E_2$ is constant and the variable changing with time is J^β.

As far as the change of C_1/C_1^0 with time is concerned, for the case of a constant potential step it has been shown that [8]

$$C_1/C_1^0 = \exp(t_n)\,\mathrm{erfc}(\sqrt{t_n}) \tag{15}$$

where t_n is the time normalized by the kinetic parameters of the process and by the value of the potential E_2, as

$$t_n = t\left[\frac{zFD^{1/2}C_1^0}{J_1^0 \exp\left[\left(\frac{\alpha_c F}{RT}\right)(E_2 - E_{r,1} + R_\Omega J^\beta)\right]}\right]^{-2} \tag{16}$$

Equation 15 is a function which decreases from the value $y = 1$ for $x = 0$ towards $y = 0$ for $x \to \infty$, but subsides to relatively low values at the value of the argument $x = 5$. Values of this function are available in the literature [9]. The change in the partial current J_1 with time is given by

$$J_1 = J_1^0[\exp(t_n)\,\mathrm{erfc}(\sqrt{t_n})] \times \exp\left[-\left(\frac{\alpha_c F}{RT}\right)(E_2 - E_{r,1} + R_\Omega J^\beta)\right] \tag{17}$$

Assuming no change in concentration of the ions of metal 2, the partial current J_2 is

$$J_2 = J_2^0 \exp\left[-\left(\frac{\alpha_c F}{RT}\right)(E_2 - E_{r,2} + R_\Omega J^\beta)\right] \tag{18}$$

The capacitive current is derived from equation (1) taking

$$E' = E_2 - E_1 + R_\Omega J^\beta \tag{19}$$

as

$$J_c = CR_\Omega \frac{dJ^\beta}{dt} = -J^\beta + J_1 + J_2 \tag{20}$$

since E_1 and E_2 are constant.

The total current J^β is the sum of the three currents given by Equations 17, 18 and 20.

Values of J^β and the three partial currents, were computed as functions of time. A typical result is shown in Figs 5 and 6 for the same set of parameters as in the galvanostatic experiment (Table 1) and for potentials varying between -0.9 and -1.6 V.

2.2. *Composition of the deposit*

The composition of the deposit resulting from the simultaneous reduction of the two metal ions, as a function of thickness of the deposited layer may be derived on the basis of the above considerations. The content of metal 1 in the deposit at any moment must be

$$x_1 = J_1/(J_1 + J_2) \tag{21}$$

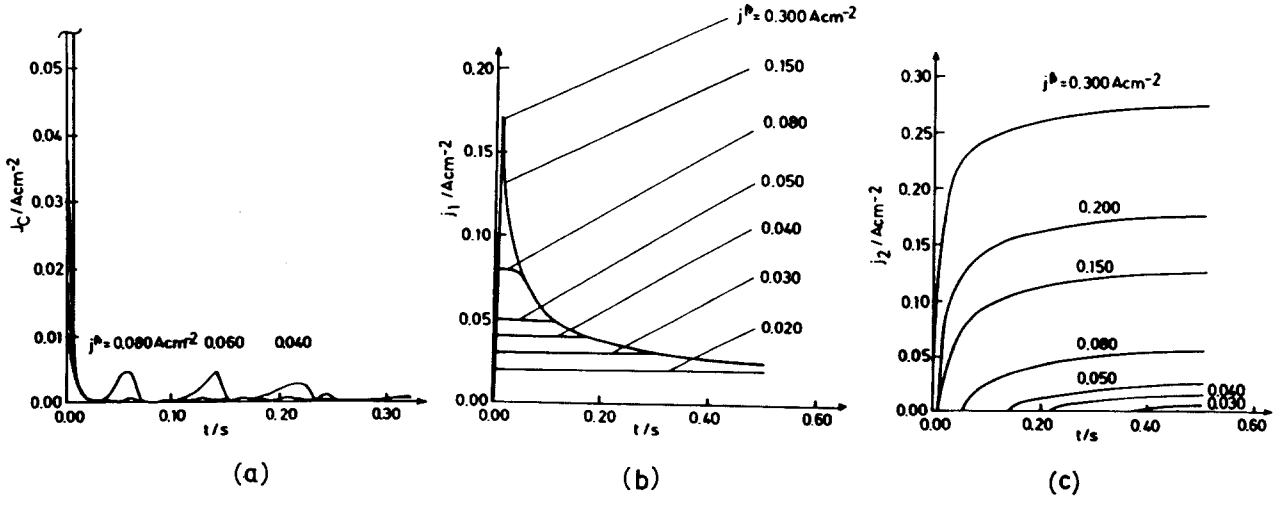

Fig. 4. Partial currents at the electrolyte/solution interface as functions of time, after imposing different constant cathodic current steps. (a) J_c: double layer charging current; (b) J_1: partial current of deposition of metal 1; (c) J_2: partial current of deposition of metal 2.

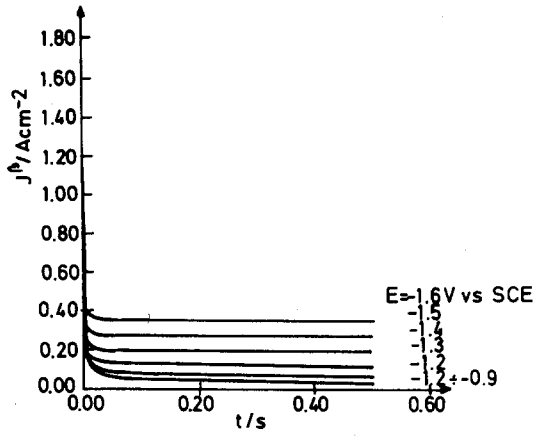

Fig. 5. Time dependence of the current density for the deposition at different constant potentials.

The thickness of the deposit at any time, assuming additivity of atomic volumes, is given by

$$\Delta = \int_0^t [(M_1/\rho_1 z_1 F)J_1 + (M_2/\rho_2 z_2 F)J_2]\,\mathrm{d}t \qquad (22)$$

Hence, the composition at each point across the deposit as a function of its growth may be expressed.

Figures 7 and 8 show typical examples of the change of composition of an alloy with thickness, when the deposition is carried out in the galvanostatic and potentiostatic mode, respectively, under the same conditions as those previously stated.

The transition layer is expected to consist of two regions of change in composition. In the first, there is a slow decrease in the content of the metal 1 and a corresponding increase in the metal 2, due to a slow change of the potential at the interface. This is due to the fact that a certain amount of electricity must pass before the interfacial capacitance is charged to new potential values needed to drive the deposition processes. However, for the usual values of the interfacial capacitance, C, and a typical ohmic resistance R_Ω, this region of deposited alloy is thin, often of the order of a monatomic layer or less and, hence, is not seen in the Figures. Thus, this part of the transition layer can be neglected. The major change in the composition occurs in the second region, which is primarily due to a slow decrease in the rate of deposition of metal 1 as a result of concentration polarization with respect to the corresponding ions. The latter follows a roughly $t^{-1/2}$ dependence to the moment when the diffusion layer boundary reaches the hydrodynamic boundary layer, whereupon the two partial currents reach their steady states and the composition becomes constant. For the galvanostatic mode of deposition the time taken for this to happen is given by Equation 10 and is seen to be independent of the deposition current. For the potentiostatic mode this may be derived by inserting J_1 from Equation 17 into Equation 8 and solving the latter for the time, τ, when $\delta = \delta_d$.

The transition layer thickness, Δ_τ, is determined by the amount of alloy which is deposited after the transition time of concentration polarization with respect to metal 1, τ', is reached and up to τ. This is dependent on the deposition current.

Δ_τ is given by Equation 22 when the integration is performed between $t = \tau'$ and $t = \tau$. (At high J^β, $\tau' \to 0$).

It is clear that the value of Δ_τ depends primarily on the hydrodynamic boundary layer created by stirring of the electrolyte (or rotation of the electrode). Figure 9 illustrates the case of galvanostatic deposition under conditions of different δ_d values, created by different rates of rotation, v, showing the dependence of the transition layer thickness on current density.

3. Experimental details

Alternate layers of copper and nickel were plated by the dual-current pulse method [5], applying such pulse trains so as to obtain deposits of ever decreasing layer thickness of equal overall thickness of about 10 μm. The depositions were carried out from a bath containing 2 M $NiSO_4.7H_2O$, 0.02 M $CuSO_4.5H_2O$, 0.5 M $C_6H_5Na_3O_7.2H_2O$. A conventional electrochemical cell with a rotating disc cathode (Tacussel–Controvit) was used. The cathode disc (4 mm diam.) was either silver or glassy carbon, polished to a mirror finish and treated in such a way that the deposit could easily be peeled off.

Three types of investigation of the deposits were carried out: (i) optical microscopic observations (stereo optical microscope, Reichert), (ii) ESCA, Auger depth profiling (Riber vacuum system) and (iii) microhardness measurements (Wolpert V-Testor 2).

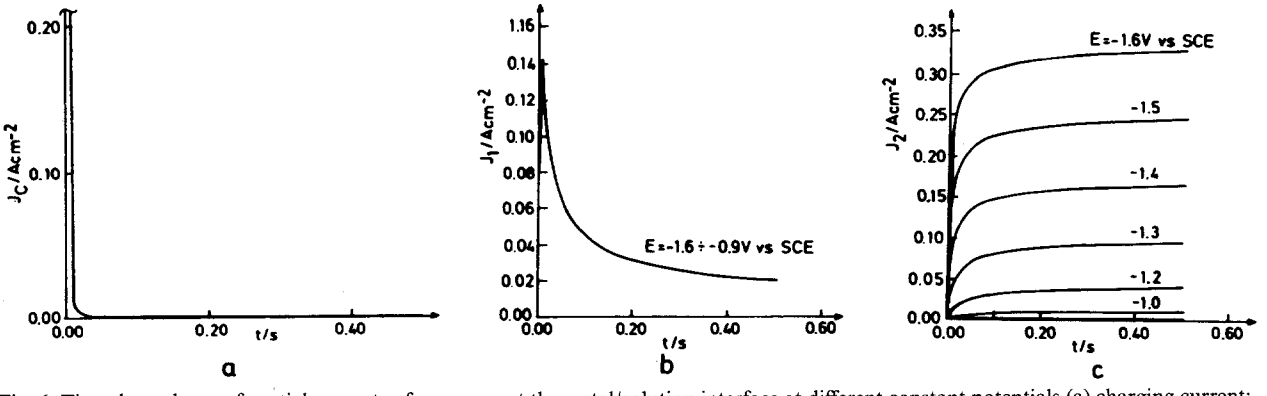

Fig. 6. Time dependence of partial currents of processes at the metal/solution interface at different constant potentials (a) charging current; (b) partial current for the deposition of metal 1; (c) partial current for the deposition of metal 2.

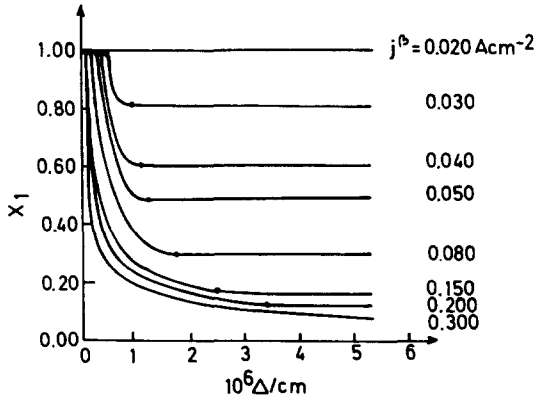

Fig. 7. The content of metal 1 as a function of thickness of layers deposited at different constant current densities.

For the optical microscopy and microhardness measurements of the cross section, the samples were embedded into an epoxy resin, cut at an angle with respect to the sample surface with a diamond saw and polished in the usual way, finishing with 0.05 μm alumina particles.

4. Results

Each of the three methods of investigation proved to be relatively suitable for a certain range of layer thickness.

4.1. *Microscopic observations*

Optical microscopy, with a maximum magnification of 2000, was used to observe layers down to thicknesses of 100 nm. Upon etching the samples, the micrographs of the cross section revealed a regular laminar structure with dark straight threads of copper interpolated between bright nickel layers. This indicated smooth deposition, layer thickness being in the range predicted by the theory for the pulse durations used in the pulse trains.

However, with further decrease in layer thickness, below 50 nm, continuity of the layers was affected. Figure 11 shows a micrograph of the surface of the deposit in such a case. Islands of the nickel alloy upon the background copper are seen rather than a continuous thin nickel layer.

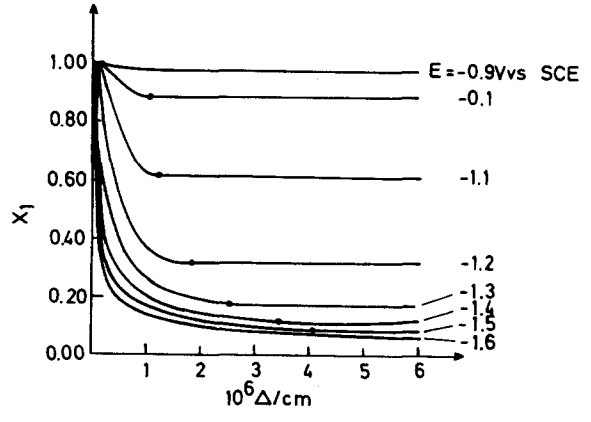

Fig. 8. The content of metal 1 as a function of thickness of layers deposited at different constant potentials.

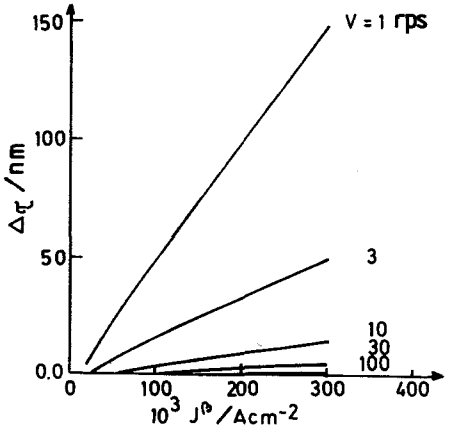

Fig. 9. Transition layer thickness as a function of deposition current density at different constant rates (rotations per second) of stirring.

4.2. *ESCA – Auger experiments*

This method proved not to be suitable for detecting thin layers of different composition. As the ion gun had a significant diameter of the beam (1 μm), by drilling a hemispherical hole which cuts through many layers, only average content of the metals could be obtained. No periodicity in composition could be observed with layers thinner than 50 nm.

4.3. *Microhardness testing*

This was done on laminar deposits obtained in the galvanostatic mode at two different current densities J^β (20 and 200 mA cm^{-2}). Layer thickness was varied by varying pulse duration. Each sample was placed in the tester and the microhardness measured at five points. Average values are shown in Fig. 12 as functions of the layer thickness.

5. Discussion

The derived relationships enable manipulation of the deposition process parameters so as to control both x_1 in the second layer and Δ_τ.

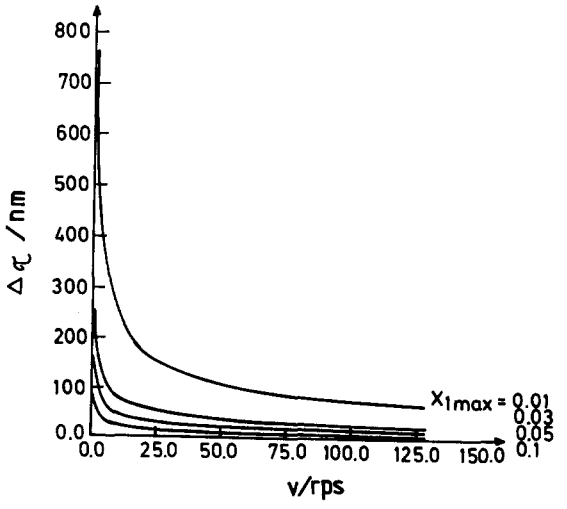

Fig. 10. Dependence of the transition layer thickness on the rate of rotation at different acceptable contents of metal 1 in the layer of metal 2.

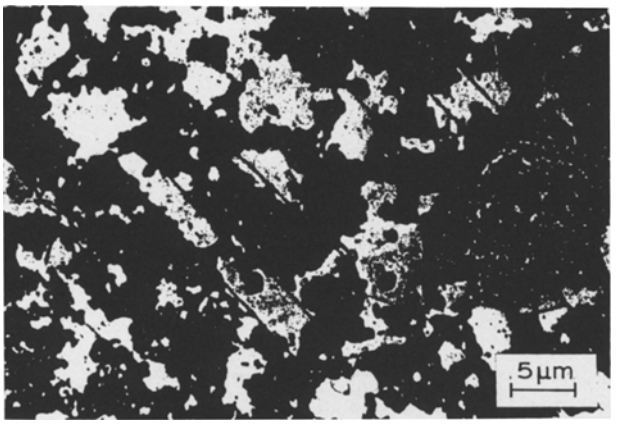

Fig. 11. Micrograph of a surface of a laminar deposit with layers 50 nm thick.

If Equation 21 is used and the charging current J_c, is neglected for the time in which pure diffusion control is established with respect to J_1, for the galvanostatic mode of operation replacing J_1 with Equation 7 and $J_1 + J_2 = J^\beta$ yields

$$x_1 = (zF\pi^{1/2}D^{1/2}C_1^0)/(2J^\beta t^{1/2}) \qquad (23)$$

The content x_1 becomes constant at the time τ given by Equation 11.

Combining Equations 23 and 11 for $t = \tau$ gives

$$x_1^\beta = zFDC_1^0/J^\beta\delta_d \qquad (24)$$

Thus the same x_1^β can be achieved by different combinations of J^β and δ_d.

On the other side, using Equations 22 and 10, an approximate relationship may be derived between J^β, δ_d and Δ_τ as

$$\Delta_\tau = J^\beta\tau = (\pi M/4zFD\rho)\delta_d^2 J^\beta \qquad (25)$$

If the maximum allowable content of the metal 1 in the second layer to $x_{1,\max}^\beta$ is fixed, from Equations 24 and 25

$$\Delta_\tau = \pi MC_1^0\delta_d/(4\rho x_{1,\max}^\beta) \qquad (26)$$

It can be seen that in such a case the thickness of the transition layer does not depend on the current density but solely on the rate of stirring, which affects δ_d. For the case of the rotating disc and combining Equation 26 with Equation 11 the dependence shown in Fig. 10 is obtained.

On the other side $x_{1,\max}^\beta$ does require a certain J^β has to be achieved within Δ_τ.

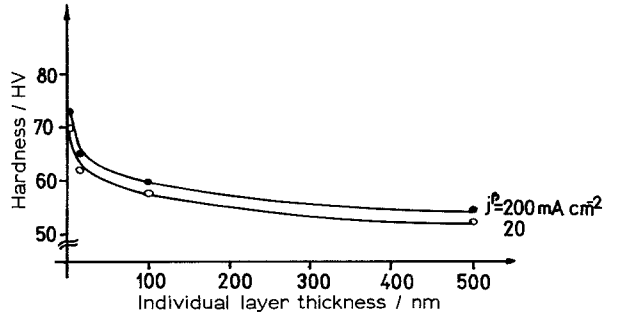

Fig. 12. Microhardness of a laminar deposit as a function of layer thickness.

From Equations 24 and 25

$$J^\beta = zF\pi DM(C_1^0)^2/(4\rho(x_{1,\max}^\beta)^2\Delta_\tau) \qquad (27)$$

Some limitations exist, however, in the choice of both J^β and δ_d. In practice, the highest J^β and v, which can be used are of order $1\,A\,cm^{-2}$ and 100 r.p.s., respectively. Hence, using Equations 11, 24 and 25, the thinnest δ_d of about 10^{-3} cm can be calculated and thus, the lowest content of the metal 1 and the thinnest transition layer, amounting to about 0.03 and 10 nm respectively. Of course, reducing J^β increases x_1^β and decreases Δ_τ while reducing v has the opposite effect, so that the choice is a matter of optimization.

Equations 24 and 25 indicate that both $x_{1,\max}^\beta$ and Δ_τ can be reduced by reducing C_1^0. This, however, also has some limitation in that the smaller it is, the lower must be J^α and the longer must be the first pulse in order to achieve a desired thickness of the layer of pure metal 1.

Results of experimental investigation sounded warning that the theory may not work beyond a certain layer thickness in which nucleation and growth phenomena start playing a dominant role.

Moreover, the observed effects on the properties of the deposit may not be due to the transition layer or the laminar structure but, rather, to a composite nature of the deposit consisting of a mixture of crystals of pure copper and of the nickel alloy, which is not normally obtained in the deposition of a homogeneous Cu–Ni alloy. Further investigation of this problem is in progress.

Acknowledgements

The authors are indebted to the Fund for Science of the Republic of Serbia whose material support made this work possible. They also wish to acknowledge the help of Ziah Burzić in obtaining results of microscopic investigation and microhardness testing as well as of Nebojša Marinković for ESCA – Auger experiments. They are also pleased to acknowledge the computing assistance of M. Dražić.

References

[1] A. Brenner, 'Electrodeposition of Alloys, Principles and Practice', Vol. 1, Academic Press, New York (1963).
[2] E. Raub and K. Muller, in "Fundamentals of Metal Deposition," Elsevier Pub. Co., New York (1967).
[3] D. S. Lashmore and O. Zadok, *J. Mater. Sci.* **22** (1987) 499.
[4] A. R. Despić and V. D. Jovic, *J. Electrochem. Soc.* **134** (1987) 3004.
[5] A. R. Despić, V. D. Jovic and S. Spaic, *J. Electrochem. Soc.* **136** (1989) 1651.
[6] A. Despić, 'Electrodeposition of Composite Structures', Plenary lecture, 31st International Congress of Pure and Applied Chemistry, Sofia, Bulgaria (1987).
[7] D. Tench and J. White, *Metall. Trans. A.* **15** (1984) 2039.
[8] H. S. Carlslaw and J. C. Jaeger, 'Conduction of Heat in Solids', Oxford University Press, London (1947) p. 373.
[9] M. Abramowitz and I. A. Stegun, 'Handbook of Mathematical Functions', National Bureau of Standards, Applied Mathematics Series 55 (1964).